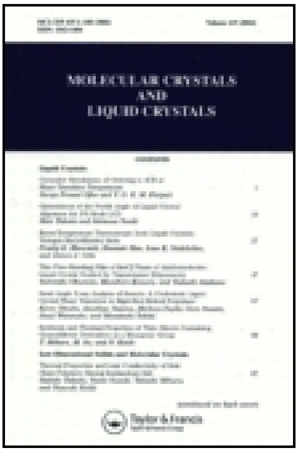

Molecular Crystals and Liquid Crystals Science and Technology. Section A. Molecular Crystals and Liquid Crystals

Publication details, including instructions for authors and subscription information:
http://www.tandfonline.com/loi/gmcl19

The Four-Wave Mixing and the Hydrodynamic Excitations in Smectic A Liquid Crystals

G. F. Kventsel [a] & B. I. Lembrikov [a]

[a] Department of Chemistry, Technion-Israel Institute of Technology, Haifa, 32000, Israel

Version of record first published: 23 Sep 2006.

Mol. Cryst. Liq. Cryst. 1995, Vol. 262, pp. 591–627
Reprints available directly from the publisher
Photocopying permitted by license only

THE FOUR-WAVE MIXING AND THE HYDRODYNAMIC EXCITATIONS IN SMECTIC A LIQUID CRYSTALS

G.F. KVENTSEL and B.I. LEMBRIKOV
Department of Chemistry, Technion–Israel Institute of Technology, Haifa 32000, Israel

Abstract A nondegenerate four-wave mixing (FWM) on a new type of Kerr nonlinearity determined by the layer deformations in smectic A liquid crystal (SmA) is considered. It is shown that in the case when the frequency difference of the coupled electromagnetic waves (EMW) is close to the frequency of the second sound (SS), a strong parametric coupling among EMW through the dynamic grating of layer deformations occurs. As a result EMW with the lowest frequency is amplified and EMW with the highest frequency is depleted, while the two EMW with the intermediate frequencies are compressed in space and their envelopes take the form of a spatial soliton. The explicit expressions of all amplitudes are calculated. The gain coefficient appears to be one order of magnitude greater than the one for stimulated scattering on an ordinary sound in organic liquids. The interaction of EMW with the specially selected frequencies and wave vectors gives rise to the analog of Brillouin enhanced FWM (BEFWM) resulting in the amplification of the phase-conjugate EMW. The additional components of the fundamental EMW and a spectrum of spatially localized Brillouin-like small harmonics with combination frequencies and wave vectors are generated due to the combined effect of the new kind of Kerr nonlinearity discussed and anisotropy of SmA. It is shown that the light generates spatially periodic hydrodynamic flow with the large-scale soliton-type envelopes. The light-induced layer deformations generate the high-frequency longitudinal electric field due to the flexoelectric effect. The spatial and temporal characteristics of the dynamic grating appears to be close to the experimental data.

1. INTRODUCTION

Four-wave mixing (FWM) refers to the nonlinear process with four interacting electromagnetic waves (EMW).[1] As a third-order process it is allowed in all media, with or without inversion symmetry.[1] The typical nonlinear optical effects caused by FWM are parametric amplification of some of the coupled EMW by the others and different techniques of the phase conjugation.[1,2] The theory of nondegenerate FWM when all frequencies of coupled EMW are different was developed for a nondissipative isotropic medium with a scalar cubic susceptibility.[3−6] The scalar character of $\chi^{(3)}$ permits a description of dynamics of the system in terms of the canonical equations for EMW intensities and to obtain in general case the exact solutions in the form of the elliptic functions.[3−6] Consequently, the energy exchange appeared to be a periodic function of the propagation distance.[6] The energy-conservation and the momentum-conservation rules for the frequencies and the wave vectors of the coupled EMW, which are necessary for an effective energy transfer from the pump waves to the amplified waves, could be met simultaneously due to the compensation of initial wave vector mismatch by the wave vector mismatch caused by the optical Kerr effect.[6] The phase conjugation takes place in the case of the degenerate or nearly degenerate FWM when all frequencies of the coupled EMW are equal, or the difference among them is small in comparison with fundamental frequencies, and when the wave vectors of the EMW are selected specifically.[1,2] A Brillouin-enhanced FWM (BEFWM) which combines the possibilities of the large phase conjugation and good energy transfer from the pump EMW to the phase-conjugate EMW occurs in the case of the nearly degenerate process due to the optical Kerr effect.[2,7−9] The optical Kerr effect, characterized by the linear dependence of the refractive index on the light intensity, is usually caused by comparatively slow processes such as Raman or Brillouin scattering, optical field-induced temperature rise in absorbing media and molecular reorientation.[1]

A strong Kerr nonlinearity due to the low energy molecular reorientation is specific to nematic liquid crystals (NLC) and smectic C liquid crytals (SmC).[11−14] The nonlinear optical effects caused by this nonlinearity were thoroughly investigated both theoretically and experimentally (see for example[11−14] and references there). Unlike NLC and SmC, in smectic A liquid crystals (SmA) a normal displacement of a layer $u(\vec{r}, t)$ is a hydrodynamic variable.[10,15−19] As a result, there exists in SmA an additional acoustic mode called a second sound (SS), which propagates without a change of mass density and represents the oscillations of a phase of the order parameter.[10,15−19] The elastic constant B associated with the layer compression is much smaller than the elastic constant associated with a bulk compression.[18] SS possesses an anisotropic dispersion relation:[10,15–18]

$$\Omega = s\,(k_{s\perp}k_{sz})\,/k_s\,, \quad s = (B/\rho)^{1/2} \tag{1}$$

Here Ω, $\vec{k}_s$, $k_{s\perp}$ and k_{sz} are the SS frequency, wave vector and its components parallel and normal to the layer plane, respectively, s is SS velocity, the Z axis is chosen to be normal to the layer plane and coincides with the SS optical axis[10] and ρ is the mass density of SmA. The light-induced smectic layer deformations represent a new mechanism of Kerr nonlinearity.[20–23]

In this paper we consider a nearly degenerate FWM in SmA due to the new mechanism of Kerr nonlinearity caused by the layer deformations. The interfering EMW create a dynamic grating of the normal layer displacement. The FWM on such a grating has two particular features. Firstly, the rules of energy-conservation and momentum-conservation for the frequencies and the wave vectors of the coupled EMW are met automatically. Secondly, the SS wave excitation can be considered highly damped due to the large viscosity of SmA.[10,16–18] Therefore, the direct energy exchange between the EMW and the rapidly decaying SS eigenmodes is negligible. As a result, the scale separation[28] is possible, and the system can be considered a nonconservative one. The energy transfer among the EMW through the dynamic grating is nonreciprocal, unlike the situation considered in ref. 3–6.

It is shown that the cubic susceptibility of the new kind caused by the dynamic grating is in general case strongly anisotropic due to the essential optical anisotropy and the spatial dispersion[24] of liquid crystals.[11–13] Usually the terms responsible for the spatial dispersion in the centrosymmetric media are of the order of magnitude of (d/λ) where d is a crystal lattice constant and λ is a light wavelength. In SmA the interlayer distance $d \sim 20\,\text{Å}$,[10] which is much greater than a cell dimension in ordinary crystals. Therefore the spatial dispersion must be more pronounced in SmA. The tensor $\chi^{(3)}_{ijkl}$ contains 10 independent components having a resonant form due to the dispersion relation (1). The components are essentially complex because of the viscosity of SmA.[10,16–18] The strong coupling occurs when the frequency differences of the coupled EMW are close to SS frequency:

$$\Delta\omega_{mn} = \omega_m - \omega_n \sim \Omega_{mn}(\Delta\,\vec{k}_{mn}) \sim \frac{s}{c}\omega_m \tag{2}$$

$$\Delta\vec{k}_{mn} = \vec{k}_m - \vec{k}_n \tag{3}$$

where $\omega_{m,n}$, $\vec{k}_{m,n}$ are the frequencies and the wave vectors of the fundamental EMW, respectively and c is the vacuum light velocity.

The condition of the resonance has the form

$$\Delta\omega_{mn} = \Omega_{mn}(\Delta\vec{k}_{mn})\ . \tag{4}$$

It is shown that the EMW with the lowest frequency is amplified with saturation, the EMW with the highest frequency is depleted, and the two EMW with the intermediate frequencies are compressed in space, forming the soliton-like envelopes.[2,25] The intensities of all EMW form the stable spatially localized nonperiodic structures. The coupled EMW undergo the phase cross-modulation along with the parametric energy exchange since the cubic susceptibility is complex. All phases evolve separately due to the anisotropic character of coupling.

In the particular case when EMW counterpropagate, an analog of BEFWM[2,4–6] is possible.

The scattering of the four fundamental EMW on the dynamic grating results in the appearence of a spectrum of small spatially localized harmonics with the combination frequencies and wave vectors. The combined effect of anisotropy and nonlinearity results in the generation of the additional components of the fundamental waves.

In SmA a time-dependent layer displacement inevitably results in the excitation of a hydrodynamic flow,[10,16–19] unlike NLC where purely orientation waves, or twist waves, are possible without any hydrodynamic motion.[10,26,27] The light-induced dynamic grating generates a hydrodynamic flow which represents a pattern oscillatory in time. It has two spatial scales: the short-scale periodicity and the large-scale soliton-type envelopes.[28] All instabilities appears to be of the convective type.[29]

The light-induced layer deformations generate the longitudinal waves[30] of the high-frequency electric field due to the flexoelectric effect specific to liquid crystals.[10,15,31]

The analysis of the nonlinear optical effects and hydrodynamics of SmA is based on the self-consistent solution of the Maxwell equations for a nonlinear inhomogeneous anisotropic medium[1] and the equation of motion of SmA in the external electric field.[20,23] We used the slowly varying amplitude (SVA) approximation and the infinite plane wave approximation.[1] The FMW in SmA is assumed to be a steady-state process.[1]

The numerical estimations show that for the typical light intensity the gain coefficient as well as the temporal and spatial characteristics of the excitations in SmA are close to the ones observed experimentally.[32-34] The article is constructed as follows: in section 2 the cubic susceptibility caused by the layer deformations is calculated; in section 3 we consider the parametric amplification, stability of the system and the analog of BEFWM; in section 4 the generation of the spectrum of the scattered harmonics and of the additional components is described; the hydrodynamics of SmA in the presence of the strong optical field is discussed in section 5. The longitudinal electric field due to the flexoelectric effect is calculated in section 6; conclusions are presented in section 7.

2. THE CUBIC NONLINEARITY CAUSED BY THE SMECTIC LAYER DEFORMATIONS.

The hydrodynamics of incompressible SmA in the external electric field $\vec{E}$ is described by the following system of equations:[10,8,24]

$$\frac{\partial v_i}{\partial x_i} = 0 \tag{5}$$

$$\rho \frac{\partial v_i}{\partial t} = -\frac{\partial P}{\partial x_i} + g_i + \frac{\partial \sigma'_{ik}}{\partial x_k} \tag{6}$$

$$\frac{\partial u}{\partial t} = v_z \tag{7}$$

$$g_{x,y} \equiv 0\ , \qquad g_z = -\frac{\delta F}{\delta u} \tag{8}$$

$$F = \frac{1}{2} B \left(\frac{\partial u}{\partial z}\right)^2 - \frac{1}{8\pi} \epsilon_{ik} E_i E_k \tag{9}$$

$$\sigma'_{ik} = \alpha_0 \delta_{ik} \mathcal{A}_{\ell\ell} + \alpha_1 \delta_{iz} \delta_{kz} \mathcal{A}_{zz} + \alpha_4 \mathcal{A}_{ik} + \alpha_{56}(\delta_{iz} \mathcal{A}_{zk} + \delta_{kz} \mathcal{A}_{zi}) + \alpha_7 \delta_{iz} \delta_{kz} \mathcal{A}_{\ell\ell} \tag{10}$$

$$\mathcal{A}_{ik} = \frac{1}{2} \left(\frac{\partial v_i}{\partial x_k} + \frac{\partial v_k}{\partial x_i}\right) \tag{11}$$

where $\vec{v}$ is the hydrodynamic velocity, P is a pressure, $\vec{g}$ is the generalized force density, F is the free energy density, σ'_{ik} is the viscous stress tensor, α_{ik} are the Leslie coefficients describing SmA viscosity, ϵ_{ik} is the dielectric constant tensor.

The X and Y axes are chosen in the plane of the layer, and the Z axis coinciding with the optical axis of SmA is normal to the layer. We neglect in (9) the small elastic terms connected with in-plane molecular deviations.[10]

The dielectric constant tensor ϵ_{ik} containing the terms linear on the layer deformations has the form:[10,17]

$$\begin{aligned} &\epsilon_{xx} = \epsilon_{yy} = \epsilon_{\perp} + a_{\perp}\frac{\partial u}{\partial z}, \quad \epsilon_{zz} = \epsilon_{\parallel} + a_{\parallel}\frac{\partial u}{\partial z}, \\ &\epsilon_{xz} = \epsilon_{zx} = -\epsilon_a \frac{\partial u}{\partial x}, \\ &\epsilon_{yz} = \epsilon_{zy} = -\epsilon_a \frac{\partial u}{\partial y} \\ &\epsilon_a = \epsilon_{\parallel} - \epsilon_{\perp} \end{aligned} \tag{12}$$

Combining the equations (5)–(12) we obtain the equation of motion of SmA in the external electric field $\vec{E}$:[20,23]

$$\begin{aligned} &-\rho\nabla^2\frac{\partial^2 u}{\partial t^2} + \left[\alpha_1\frac{\partial^2}{\partial z^2}\nabla_{\perp}^2 + \frac{1}{2}(\alpha_4+\alpha_{56})\nabla^2\nabla^2\right]\frac{\partial u}{\partial t} + B\frac{\partial^2}{\partial z^2}\nabla_{\perp}^2 u = \\ &= \frac{1}{8\pi}\nabla_{\perp}^2\left\{\frac{\partial}{\partial z}\left(a_{\perp}E_{\perp}^2 + a_{\parallel}E_z^2\right) - 2\epsilon_a\left[\frac{\partial}{\partial x}(E_zE_x) + \frac{\partial}{\partial y}(E_zE_y)\right]\right\} \end{aligned} \tag{13}$$

where

$$\nabla_{\perp} = \vec{x}\frac{\partial}{\partial x} + \vec{y}\frac{\partial}{\partial y}\ ; \qquad \vec{E}_{\perp} = \vec{x}E_x + \vec{y}E_y \tag{14}$$

We use the infinite plane wave and SVA approximations[1] and write the electric fields of the four fundamental EMW in the form:

$$\vec{E}_m = \vec{e}_m\left\{A_m(z)\exp i(\vec{k}_m\vec{r} - \omega_m t) + c.c.\right\}\ , \qquad m = 1, \ldots, 4 \tag{15}$$

where $\vec{e}_m$ are the polarization unit vectors, the frequencies ω_m satisfy the condition (3), c.c. means complex conjugate, and the amplitudes

$$A_m = |A_m|\exp i\gamma_m$$

are slowly varying

$$\left|\frac{\partial^2 A_m}{\partial z^2}\right| << \left|k_m\frac{\partial A_m}{\partial z}\right| \tag{16}$$

We suppose that all waves (15) propagate from the free semi-space $z < 0$ into the SmA filling the semi-space $z > 0$. For the sake of definiteness we assume that

$$\omega_1 < \omega_2 < \omega_3 < \omega_4 \tag{17}$$

SmA is a uniaxial crystal,[10] and therefore the waves (15) would propagate in it as the ordinary or extraordinary ones, depending on their polarization.[24] An ordinary EMW is polarized normal to incidence plane and has the following polarization vector $\vec{e}_m^{\,o}$ and dispersion relation:[24]

$$\vec{e}_m^{\,o} = \vec{e}_{m\perp}^{\,o} = (e_{mx}, e_{my}, 0) \ , \qquad k_m^2 = \left(\frac{\omega_m}{c}\right)^2 \epsilon_\perp \tag{18}$$

An extraordinary EMW is polarized in the incidence plane and its polarization vector $\vec{e}_m^{\,e}$ and dispersion relation have the form:[24]

$$\vec{e}_m^{\,e} = (\vec{e}_{m\perp}^{\,e}, e_{mz}^e) \ , \qquad \frac{k_{m\perp}^2}{\epsilon_\parallel} + \frac{k_{mz}^2}{\epsilon_\perp} = \left(\frac{\omega_m}{c}\right)^2 \tag{19}$$

where

$$\vec{k}_{m\perp} = \vec{x} k_{mx} + \vec{y} k_{my}$$

In general case an arbitrary polarized EMW splits into an ordinary EMW and an extraordinary one,[24] which results in the eight-wave mixing instead of FWM. This case is not considered.

In our case the incidence plane containing the optical axis Z coincides with the main cross-section.[24] We consider separately the cases of the interaction of the extraordinary and ordinary EMW. The interaction of the EMW with both types of polarization differs only by the form of coupling constants. First consider the coupling of the extraordinary EMW. Substituting (15) and (19) into (13) and keeping only the terms with the difference frequencies (3) we obtain the inhomogeneous part of solution of (13) governed by the field terms in the right-hand side of the equation of motion (13):

$$u(\vec{r}, t) = \sum_{m,\, n,\, m \neq n} U_{mn} \exp i \left(\vec{k}_{mn} \vec{r} - \Delta\omega_{mn} t \right) \tag{20}$$

$$U_{mn} = \frac{i}{4\pi\rho} \left(\frac{\Delta k_{mn\perp}}{\Delta k_{mn}} \right)^2 A_m A_n^* \frac{h_{mn}}{G_{mn}} \tag{21}$$

$$h_{mn} = \left\{a_\perp (\vec{e}_{m\perp}\vec{e}_{n\perp}) + a_\| (e_{mz}e_{nz})\right\} \Delta k_{mnz} - \\ - \epsilon_a \left\{e_{mz}\left(\Delta\vec{k}_{mn\perp}\vec{e}_{n\perp}\right) + e_{nz}\left(\Delta\vec{k}_{mn\perp}\vec{e}_{m\perp}\right)\right\} \tag{22}$$

$$G_{mn} = (\Delta\omega_{mn})^2 - \Omega^2_{mn} + i\Delta\omega_{mn}\Gamma_{mn} \tag{23}$$

$$\Omega^2_{mn} = s^2 \frac{(\Delta k_{mn\perp}\Delta k_{mnz})^2}{(\Delta k_{mn})^2} \tag{24}$$

$$\Gamma_{mn} = \frac{1}{\rho}\left[\alpha_1 \left(\frac{\Delta k_{mn\perp}\Delta k_{mnz}}{\Delta k_{mn}}\right)^2 + \frac{(\alpha_4 + \alpha_{56})}{2}(\Delta k_{mn})^2\right] \tag{25}$$

Ω_{mn} and Γ_{mn} have the meaning of a frequency and a temporal decay constant of SS eigenmode. The constant h_{mn} contains the polarization dependence, and in the case of the mixing of ordinary waves it takes the form

$$h^o_{mn} = a_\perp \Delta k_{mnz} (\vec{e}_{m\perp}\vec{e}_{n\perp}) \tag{26}$$

It is seen from the expressions (21) and (26) that the mixing of the ordinary waves may be polarization-decoupled,[8] if $\vec{e}_{m\perp} \perp \vec{e}_{n\perp}$, which is impossible in the case of the mixing of extraordinary waves.

The contribution of the static layer deformations

$$\left(\frac{\partial u_m}{\partial z}\right)_{stat} \sim \frac{a_\perp}{4\pi B}|A_m|^2$$

may be neglected, since for $(\Delta\omega_{mn})^2 \sim \Omega^2_{mn}$

$$\left|\frac{\partial u_{mn}}{\partial z}\right| \sim \frac{a_\perp}{4\pi B}\frac{|A_m A_n| h_{mn}\Omega^2_{mn}}{|G_{mn}|\Delta k_{mnz}} >> \left|\frac{\partial u_m}{\partial z}\right|_{stat} \tag{27}$$

The rapidly decaying homogeneous solution of the equation (13) may also be neglected.

The layer displacement (20) represents the dynamic grating consisting of 6 harmonics caused by the interference of the fundamental EMW (15).

Substituting the relationships (20)-(22) into (12) one may see that the non-linear part of ε_{ik} caused by optical field-induced deformations may be expanded in terms of the products of the coupled waves as follows:

$$\varepsilon^N_{ik} = \sum_{m,\,n,\,m\neq n} \left(\chi^{(3)}_{mn}\right)_{ijk\ell} (e_m)_j (e_n)_\ell A_m A^*_n \times \exp i\left(\Delta\vec{k}_{mn}\vec{r} - \Delta\omega_{mn} t\right) \tag{28}$$

where the coefficients of the expansion $\left(\chi_{mn}^{(3)}\right)_{ijk\ell}$ represent fourth rank tensor of the cubic susceptibility determined by the dynamic grating (20). It is seen from (28) that ε_{ik}^{N} is a superposition of all possible two-wave mixing terms with the frequency difference (3). The explicit expressions of $\left(\chi_{mn}^{(3)}\right)_{ijk\ell}$ are presented in Appendix A. In general,

$$\left(\chi_{mn}^{(3)}\right)_{ijk\ell} \sim S_{mn}(\Delta k_{mn})_j(\Delta k_{mn})_\ell \tag{29}$$

and contains the factors describing the spatial dispersion[24] (dependence on the wave vector $\Delta\vec{k}_{mn}$ of the dynamic grating) and the resonant factor S_{mn}

$$S_{mn} = \frac{1}{4\pi\rho G_{mn}}\left(\frac{\Delta k_{mn\perp}}{\Delta k_{mn}}\right)^2 \tag{30}$$

The resonance occurs if

$$\Delta\omega_{mn} = s\frac{\Delta k_{mn\perp}\Delta k_{mnz}}{\Delta k_{mn}} \tag{31}$$

$\left(\chi_{mn}^{(3)}\right)_{ijk\ell}$ is essentially complex, and it is seen from (23) and (30) that

$$\left(\chi_{mn}^{(3)}\right)_{ijk\ell} = \left(\chi_{nm}^{(3)}\right)^*_{ijk\ell} \tag{32}$$

It is seen from the expressions (28) and (29) that each term in the series ε_{ik}^{N} includes both the spatial dispersion and nonlinearity factor.

In the framework of the essentially nonlinear theory the field in a nonlinear medium is described by the wave equation[1]

$$\text{rot rot}\vec{E} + \frac{1}{c^2}\frac{\partial^2\vec{D}^L}{\partial t^2} = -\frac{1}{c}\frac{\partial^2\vec{D}^N}{\partial t^2} \tag{33}$$

$$\vec{D}_\perp^L = \varepsilon_\perp\vec{E}_\perp, \quad D_z^L = \varepsilon_\parallel E_z, \quad D_i^N = \varepsilon_{ik}^N E_k \tag{34}$$

$$\vec{E} = \sum_{m=1}^{4}\vec{E}_m + \sum_\ell \vec{f}_\ell^s + c.c. \tag{35}$$

where $\vec{E}$ is the total electric field in SmA, $\vec{f}_\ell^s$ are the small scattered harmonics with the combination frequencies and wave vectors, $\vec{D}^L$ and $\vec{D}^N$ are the linear and the nonlinear parts of the electric induction, respectively.

Comparison of the relationships (2), (3), (12), (15), (28) and (33)–(35) shows that the nonlinear part of the electric induction $\vec{D}^N$ consists of 48 terms with the essentially different phases:

$$\vec{D}^N = \sum_{\ell=1}^{48} \left(\vec{D}_\ell^N \exp i\psi_\ell + c.c. \right) \tag{36}$$

The amplitudes D_ℓ^L are essentially complex according to (28)–(30) and (34). Consequently in the system considered the EMW amplification and phase cross-modulation are possible.[12] On the other hand, the stable soliton-like excitations would occur without a threshold since the spatial dispersion terms and the non-linear terms are identical.[25] The energy and momentum-conservation rules for the frequencies and wave vectors of the fundamental EMW are met automatically in the case of the scattering on the dynamic grating (20). As a result each fundamental EMW and three nonlinear terms of the series (36) are phase-matched.

In general case the phase-matched terms $\vec{D}_\ell^N$ are not parallel to the electric fields $\vec{E}_m$ of the corresponding EMW due to the anisotropy of SmA, as it is seen from the relationships (12) and (34). The components of $\vec{D}_\ell^N$ which are parallel to the corresponding field contribute to the energy exchange between the waves, while the components which are normal to the field generate the additional components of the fundamental fields. Other 36 terms of the series (33) give rise to the scattered harmonics $\vec{f}_\ell^s$. As a result, we obtain from the wave equation (33) three kinds of equations.

1. The reduced equations for the SVA of the fundamental EMW (15) with the parallel components of the phase-matched terms $\vec{D}_\ell^N$ in the right-hand side.
2. The wave equations for the additional components of the fundamental EMW fields with the normal components of the phase-matched terms $\vec{D}_\ell^N$ in the right-hand side.
3. The wave equations for the scattered harmonics $\vec{f}_\ell^s$ with the terms $\vec{D}_\ell^N$ in the right-hand side which are not phase-matched to the fundamental EMW.

3. THE PARAMETRIC AMPLIFICATION AND THE PHASE CONJUGATION.

Substituting the expressions (15) and (34)–(36) into the wave equation (33), choosing the phase-matched terms in the left-hand side and the right-hand side of the equation (33), projecting the corresponding nonlinear induction vectors on the fundamental wave field directions, taking into account the conditions (16) and (18) or (19) for each type of polarization and separating the real and the imaginary parts, we obtain two sets of the reduced equations for the moduli $|A_m|$ and the phases γ_m of the SVA. They have the form:

$$-l_m\left(\frac{\omega_m}{c}\right)^{-2}\frac{\partial|A_m|^2}{\partial z}=|A_m|^2\sum_n\frac{h_{mn}^2|A_n|^2}{4\pi\rho}\times\left(\frac{\Delta k_{mn\perp}}{\Delta k_{mn}}\right)^2\frac{\Delta\omega_{mn}\Gamma_{mn}}{|G_{mn}|^2} \tag{37}$$

$$-2l_m\frac{\partial\gamma_m}{\partial z}=\left(\frac{\omega_m}{c}\right)^2\sum_n\frac{h_{mn}^2|A_n|^2\left\{(\Delta\omega_{mn})^2-\Omega_{mn}^2\right\}}{4\pi\rho|G_{mn}|^2}\times\left(\frac{\Delta k_{mn\perp}}{\Delta k_{mn}}\right)^2 \tag{38}$$

where $m,\ n=1,\ldots,4$

$$l_m=k_{mz}^o,\quad \text{or}\quad k_{mz}^e\left\{1-e_{mz}^e\left(\vec{k}_m^e\vec{e}_m^e\right)/k_{mz}^e\right\}$$

for the ordinary and the extraordinary EMW, respectively.

3.1. The General Case.

Consider first the system of equations (37). The system has only one integral of motion which is immediately obtained using the conditions (3), and (22)–(25).

$$\sum_{m=1}^4 l_m\left(\omega_m/c\right)^{-2}|A_m|^2=\text{const}=I_0 \tag{39}$$

Introducing the dimensionless variables

$$W_m=l_m\left(\omega_m/c\right)^{-2}|A_m|^2/I_0,\quad \sum_{m=1}^4 W_m=1 \tag{40}$$

we transform the equations (37) and (38) as follows:

$$-\frac{\partial(\ln W_m)}{\partial z}=\sum_n\beta_{mn}W_n,\quad m\neq n \tag{41}$$

$$-\frac{\partial\gamma_m}{\partial z}=\frac{1}{2}\sum_n\delta_{mn}W_n,\quad m\neq n \tag{42}$$

where

$$\beta_{mn}=\left[\frac{\omega_m\omega_n}{c^2}\right]^2\frac{I_0h_{mn}^2\Delta\omega_{mn}\Gamma_{mn}}{4\pi\rho|G_{mn}|^2l_ml_n}\left(\frac{\Delta k_{mn\perp}}{\Delta k_{mn}}\right)^2 \tag{43}$$

$$\delta_{mn}=\left[\frac{\omega_m\omega_n}{c^2}\right]^2\frac{I_0h_{mn}^2\left[(\Delta\omega_{mn})^2-\Omega_{mn}^2\right]}{4\pi\rho|G_{mn}|^2l_ml_n}\left(\frac{\Delta k_{mn\perp}}{\Delta k_{mn}}\right)^2 \tag{44}$$

The analytical solution of the system (41) is hardly possible, although the behaviour of the solution may be evaluated qualitatively. The conditions (3) and (17) result in the following properties of the coupling constants

$$\begin{aligned} \beta_{mn} = -\beta_{nm}, \quad \beta_{mn} &> 0, \quad m > n, \\ \beta_{mn} &< 0, \quad m < n \end{aligned} \tag{45}$$

Taking into account (45) we obtain that

$$\frac{\partial W_1}{\partial z} > 0, \quad \frac{\partial W_4}{\partial z} < 0$$

while $\partial W_{2,3}/\partial z$ may change sign. Consequently, the intensity W_1 of the wave with the lowest frequency ω_1 increases monotonously, the intensity W_4 of the wave with the greatest frequency ω_4 decreases monotonously, while the intensities $W_{2,3}$ of the waves with the intermediate frequencies $\omega_{2,3}$ may have their extrema at $z > 0$. For

$$\beta_{42} W_4(0) + \beta_{32} W_3(0) > \beta_{21} \cdot W_1(0) \tag{46}$$

W_2 has a maximum at the point

$$z = z_{02} > 0$$

where

$$\beta_{42} W_4(z_{02}) + \beta_{32} W_3(z_{02}) = \beta_{21} W_1(z_{02}) \tag{47}$$

Similarly, for

$$\beta_{43} W_4(0) > \beta_{31} W_1(0) + \beta_{32} W_2(0) \tag{48}$$

W_3 has a maximum at the point

$$z = z_{03} > 0$$

where

$$\beta_{43} W_4(z_{03}) = \beta_{31} W_1(z_{03}) + \beta_{32} W_2(z_{03}) \tag{49}$$

For the opposite signs in inequalities (46) and (48) the solutions $z_{02,03} > 0$ do not exist, and $W_{2,3}$ monotonously decrease just like W_4 does.

The system (41) has the formal solution

$$W_m = W_m(0) \exp \int_0^z \left\{ -\sum_n \beta_{mn} W_n dz' \right\} \tag{50}$$

Taking into account the behaviour of W_1 we immediately obtain from (50) that

$$W_{2,3,4}(z \to \infty) \to 0 \tag{51}$$

The integrand in the exponent of W_1 vanishes exponentially at infinity, while the intergration interval increases linearly. Therefore W_1 tends to the finite constant level as $z \to \infty$. Taking into account the conditions (40) and (51), we obtain

$$W_1(z \to \infty) \to 1 \tag{52}$$

The results (51) and (52) show that the parametric amplification with saturation of the signal wave E_1 occurs while the pumping wave E_4 undergoes total depletion in the limit $z \to \infty$. The intensities of the waves $E_{2,3}$ with the intermediate frequencies form the spatially localized soliton-like states, if the pumping wave E_4 at the input $z = 0$ is sufficiently strong to satisfy the conditions (46) and (48). In the excitation interval $min(z_{02}, z_{03}) > z > 0$ three waves $E_{1,2,3}$ are amplified. The solutions (50) are nonperiodical and stable as $z \to \infty$.

The coupling constants β_{mn} play a role of the gain coefficients and reach their maximal values in the case of the resonance. Taking into account the relationships (1)–(4), (18) or (19), (22)–(25), (40) and (43) we obtain

$$\begin{aligned} |\beta_{mn}^{res}| = \left[\frac{\omega_m \omega_n}{c^2}\right]^2 \frac{I_0 h_{mn}^2 |\Omega_{mn}|}{4\pi B (\Delta k_{mnz})^2 l_m l_n \Gamma_n} \sim \\ \sim \frac{\omega_m}{c^2} \frac{\mathcal{P}}{B} \frac{\varepsilon_a^2}{\sqrt{\varepsilon_\perp \varepsilon_\parallel}} \frac{|\Omega_{mn}|}{\Gamma_{mn}} \end{aligned} \tag{53}$$

where the intensity $\mathcal{P}$ has the form:[24]

$$\mathcal{P} = c|A|^2/4\pi$$

At the frequency $\omega_m \sim 10^{15}\,\text{sec}^{-1}$ for the typical values of the material parameters $\varepsilon_\perp = 2.3$, $\varepsilon_\parallel = 2.9$, $\varepsilon_a = 0.6$,[13] $B \sim 10^8\,\text{erg/cm}^3$, $\alpha_i \sim (0.3 - 1)$ Poise,[10,18,40,41] for the small angles between $\vec{k}_m$ and $\vec{k}_n$ ($\theta \sim 1°$)[32] the gain coefficient per unit intensity is estimated to be

$$\frac{\beta}{\mathcal{P}} \sim (0.15 - 0.5) \text{ cm } (MW)^{-1}$$

which is comparable with the gain coefficient for the Brillouin scattering in CS_2 and at least of one order of magnitude greater than the gain coefficients for other organic liquids.[1]

The behaviour of the phases γ_m is described by the following solutions:

$$\gamma_m - \gamma_m(0) = -\frac{1}{2}\int_0^z \sum_n \delta_{mn} W_n dz' \qquad (54)$$

It is seen from the systems (42) and (54) that each phase evolves independently, unlike the situation when a cubic susceptibility is a scalar.[6] In general case each phase shift may be positive, or negative.

If for all m, n

$$(\Delta\omega_{mn})^2 > \Omega^2_{mn}$$

then all phase shifts are negative, i.e. a medium is defocusing.[1] In the opposite case

$$(\Delta\omega_{mn})^2 < \Omega^2_{mn}$$

all phase shifts are positive, and the medium is focusing.[1] The resonant pair of EMW does not contribute to the right-hand side of (42) since

$$\delta^{res}_{mn} = 0$$

One may see from the equations (43), (44), (50), (53) and (54) that the parametric energy exchange is predominant in comparison with the weak phase cross-modulation when

$$(\Delta\omega_{mn})^2 \sim \Omega^2_{mn}, \quad \frac{\left|(\Delta\omega_{mn})^2 - \Omega^2_{mn}\right|}{(\Delta\omega_{mn})^2} << 1$$

and consequently

$$|\delta_{mn}| << |\beta_{mn}|$$

It is instructive to conclude this section with a few general remarks.

The energy exchange among the coupled EMW is nonreciprocal unlike the situation in the conservative system.[6] The system considered has only one integral of motion (39) because the direct energy exchange between the optical field and SS is neglected. Such an approximation is valid, if the dissipation length of the SS mode

$$L_{Dmn} = s\Gamma_{mn}^{-1}$$

is small in comparison with the excitation length[28] of a virtual SS mode

$$L_{Emn} = |\beta_{mn}|^{-1} \tag{55}$$

In our case there exist 6 excitation lengths which may be also defined as the correlation lengths for each pair of the coupled EMW E_m and E_n. Using (53) one may see that

$$L_{Dmn}/L_{Emn} << 1$$

Consequently, SS modes are passive, or "slaved", and the scale separation exists between the dissipation and the excitation processes.[28] The system may be characterized as quasi-dissipative, and the dynamic grating (20) plays a role of an elastic channel for the nonreciprocal energy exchange among the coupled EMW on the distances of the order of magnitude of the excitation length L_{Emn}.

In strong optical fields with intensities $\mathcal{P} \sim 100\,\text{MW/cm}^2$ which were used in the excitation of the ultrasonic waves in SmA[32,33] the excitation length reaches $(0.02 - 0.07)$ cm according to the expressions (53) and (55). This result is in accordance with the experimental data.[33]

3.2. Polarization-decoupled FWM.

FWM is polarization-decoupled, when some of coupled EMW have perpendicular polarizations.[8] Comparing the relationships (22), (26) and (43) one may see that polarization-decoupled FWM is possible for the ordinary EMW, since such waves with perpendicular polarizations do not excite the dynamic grating, and corresponding coupling constant vanishes. In the case of extraordinary waves polarization decoupling is impossible because of anisotropy. If each EMW is polarized normal to its incidence plane and therefore propagates as an ordinary one[24] and one field is perpendicular to the others (for example $\vec{E}_1 \perp \vec{E}_{2,3,4}$), then substituting (26) into (43) we find:

$$\begin{gathered}\beta_{12} = \beta_{13} = \beta_{14} = 0 \\ W_1 = \text{const}, \quad \gamma_1 = \text{const}\end{gathered} \tag{56}$$

The critical point z_{02} vanishes, W_2 increases monotonously with saturation as $z \to \infty$, W_4 is depleted in the same way as in the general case, and W_3 has a soliton-like form with a maximum at

$$z = z_{03}$$

The signal wave polarized normal to all other waves propagates through the nonlinear medium without any change.

If

$$\vec{E}_1 \perp \vec{E}_{2,3}, \quad \vec{E}_1 \parallel \vec{E}_4$$

then

$$\begin{gathered}\beta_{12} = \beta_{13} = \beta_{24} = \beta_{34} = 0 \\ \delta_{12} = \delta_{13} = \delta_{24} = \delta_{34} = 0\end{gathered} \tag{57}$$

The equations (41)–(42) now take the form:

$$\frac{\partial W_{1,4}}{\partial z} = \pm\beta_{41} W_1 W_4 \tag{58a}$$

$$\frac{\partial W_{2,3}}{\partial z} = \pm\beta_{32} W_2 W_3 \tag{58b}$$

$$\begin{gathered}-\frac{\partial \gamma_{1,4}}{\partial z} = \frac{1}{2}\delta_{14} W_{4,1}, \\ -\frac{\partial \gamma_{2,3}}{\partial z} = \frac{1}{2}\delta_{32} W_{3,2}\end{gathered} \tag{59}$$

The equations (58), (59) describe two independent processes of two-wave mixing.[23] The solution has the form:[23]

$$\begin{gathered}W_{1,4} = \frac{1}{2} J_1 \left\{1 \pm \tanh\left[\frac{1}{2} J_1 \beta_{41} (z - z_1)\right]\right\} \\ J_1 = W_1(0) + W_4(0), \quad z_1 = \frac{1}{\beta_{41} J_1} \ln\left\{W_4(0)/W_1(0)\right\}\end{gathered} \tag{60}$$

$$W_{2,3} = \frac{1}{2}J_2\left\{1 \pm \tanh\left[\frac{1}{2}J_2(z-z_2)\beta_{32}\right]\right\}$$
$$J_2 = W_2(0) + W_3(0), \quad z_2 = \frac{1}{\beta_{32}J_2}\ln\left\{W_3(0)/W_2(0)\right\} \tag{61}$$

$$J_1 + J_2 = 1 \tag{62}$$

$$\gamma_1 + \gamma_4 = -\frac{1}{2}\delta_{14}J_1 z + \text{const}_1 \tag{63a}$$

$$\gamma_2 + \gamma_3 = -\frac{1}{2}\delta_{32}J_2 z + \text{const}_2 \tag{63b}$$

$$\gamma_1 = \gamma_1(0) - \frac{\delta_{14}}{2}z + \frac{\delta_{14}}{\beta_{41}}\ln\left\{\frac{\cosh[J_1\beta_{41}(z-z_1)/2]}{\cosh[J_1\beta_{41}z_1/2]}\right\} \tag{64}$$

$$\gamma_3 = \gamma_3(0) - \frac{\delta_{32}}{2}z + \frac{\delta_{32}}{\beta_{32}}\ln\left\{\frac{\cosh[J_2\beta_{32}(z-z_2)/2]}{\cosh[J_2\beta_{32}z_2/2]}\right\} \tag{65}$$

The expressions (60) and (61) represent two independent pairs of kinks[25] with the different crossing-points $z_{1,2}$ and excitation lengths

$$L_1 = (\beta_{41})^{-1}, \qquad L_2 = (\beta_{32})^{-1}$$

The crossing-points $z_{1,2}$ exist, if

$$W_4(0) > W_1(0), \qquad W_3(0) > W_2(0)$$

respectively.

3.3. The Stability Analysis in the Case of the Strong Pumping.

Consider the important case, when the pumping wave $\vec{E}_4$ and the signal wave $\vec{E}_1$ are much stronger than $E_{2,3}$ which play a role of idler waves:

$$W_{1,4} >> W_{2,3} \tag{66}$$

Using the expansions

$$W_1 = W_{10} + W_{11} + \dots, \quad W_4 = W_{40} + W_{41} + \dots$$
$$W_{10} >> W_{11}, \quad W_{40} >> W_{41} \tag{67}$$

and taking into account (66) and (67) we obtain from the system (41)

$$\frac{\partial W_{10,40}}{\partial z} = \pm\beta_{41}W_{10}W_{40} \tag{68}$$

$$\frac{\partial W_2}{\partial z} = W_2 \{\beta_{42} W_{40} - \beta_{21} W_{10}\} \tag{69}$$

$$\frac{\partial W_3}{\partial z} = W_3 \{\beta_{43} W_{40} - \beta_{31} W_{10}\} \tag{70}$$

$$\frac{\partial W_{11}}{\partial z} = W_{10} \{\beta_{21} W_2 + \beta_{31} W_3\} + \beta_{41} W_{40} W_{11} + \beta_{41} W_{41} W_{10} \tag{71}$$

$$\frac{\partial W_{41}}{\partial z} = -W_{40} \{\beta_{42} W_2 + \beta_{43} W_3\} - \beta_{41} W_{10} W_{41} - \beta_{41} W_{11} W_{40} \tag{72}$$

The equations (68) and (58a) have the same solution (60). Solving the equations (69)–(72) we find the separate integral of motion:

$$W_2 + W_3 + W_{11} + W_{41} = \text{const} \tag{73}$$

It is clear that

$$W_{11}(0) = W_{41}(0) = 0 \tag{74}$$

Therefore the integral of motion (73) is equal to J_2, and the condition (62) is held. All functional determinants of the system (69)–(72) are equal to zero, and as a result it has an infinite number of solutions.[35] However, the physically meaningful solutions must satisfy the conservation law (73). The intensities $W_{2,3}$ are calculated by substitution of the expressions (60) into the equations (69) and (70). They have the form:

$$W_2 = W_2(0) \exp(a_1 \eta) \left[\frac{\cosh(\eta_1)}{\cosh(\eta - \eta_1)}\right]^{b_1} \tag{75}$$

$$W_3 = W_3(0) \exp(a_2 \eta) \left[\frac{\cosh(\eta_1)}{\cosh(\eta - \eta_1)}\right]^{b_2} \tag{76}$$

where

$$\begin{aligned} \eta = \frac{\beta_{41}}{2} J_1 z, \quad a_1 &= \frac{\beta_{42} - \beta_{21}}{\beta_{41}}, \quad b_1 = \frac{\beta_{42} + \beta_{21}}{\beta_{41}} \\ a_2 &= \frac{\beta_{43} - \beta_{31}}{\beta_{41}}, \quad b_2 = \frac{\beta_{43} + \beta_{31}}{\beta_{41}} \end{aligned} \tag{77}$$

It is seen from the relationships (75)–(77) that

$$|a_1| < |b_1|, \quad |a_2| < |b_2|, \quad b_{1,2} > 0$$

and consequently

$$\eta \to \infty, \qquad W_{2,3} \to 0 \tag{78}$$

which coincides with the general result (51). If $a_{1,2} > 0$, a slow decay of $W_{2,3}$ occurs, in the opposite case $a_{1,2} < 0$ the decay of $W_{2,3}$ is rapid.

The analysis shows that $W_{2,3}$ reach their maxima at the points $z_{02,03}$, respectively, which are determined by the following expressions:

$$z_{02} = \frac{1}{\beta_{41} J_1} \ln \left[\frac{\beta_{42} W_4(0)}{\beta_{21} W_1(0)} \right] \tag{79a}$$

$$z_{03} = \frac{1}{\beta_{41} J_1} \ln \left[\frac{\beta_{43} W_4(0)}{\beta_{31} W_1(0)} \right] \tag{79b}$$

The solutions $z_{02} > 0$, $z_{03} > 0$ exist, if

$$\frac{\beta_{42} W_4(0)}{\beta_{21} W_1(0)} > 1, \qquad \frac{\beta_{43} W_4(0)}{\beta_{31} W_1(0)} > 1 \tag{80}$$

Suppose that the crossing-point $z_1 > 0$ exists and

$$\frac{\beta_{42}}{\beta_{21}} < 1, \qquad \frac{\beta_{43}}{\beta_{31}} < 1$$

Then the threshold values of the input pumping-signal ratio exist such that

$$z_{02} = z_{03} = 0$$

the spatial solitons are absent and $W_{2,3}$ decrease monotonously:

$$\left[\frac{W_4(0)}{W_1(0)} \right]_2^{tr} = \frac{\beta_{21}}{\beta_{42}}, \qquad \left[\frac{W_4(0)}{W_1(0)} \right]_3^{tr} = \frac{\beta_{31}}{\beta_{43}}$$

For the larger values of the input pumping-signal ratio the spatial solitons (75) and (76) emerge which are localized in the excitation interval

$$0 < z_{02,03} < z_1$$

(the rapid decay). If on the contrary

$$\frac{\beta_{43}}{\beta_{31}} > \frac{\beta_{42}}{\beta_{21}} > 1$$

then

$$z_{03} > z_{02} > z_1$$

and the spatial solitons $W_{2,3}$ are "pushed" forward from the excitation interval $z_1 > z > 0$ (slow decay regime). Substituting the expressions (79 a,b) into (75), (76) and using (60), (77) we find:

$$W_{2max} = W_2(0) \left[\frac{\beta_{42} W_4(0)}{\beta_{21} W_1(0)} \right]^{\frac{a_1}{2}} \left\{ \frac{J_1}{(\beta_{21} + \beta_{42})} \sqrt{\frac{\beta_{42}\beta_{21}}{W_4(0) W_1(0)}} \right\}^{b_1} \tag{81a}$$

$$W_{3max} = W_3(0) \left[\frac{\beta_{43} W_4(0)}{\beta_{31} W_1(0)} \right]^{\frac{a_2}{2}} \left\{ \frac{J_1}{(\beta_{31} + \beta_{43})} \sqrt{\frac{\beta_{43}\beta_{31}}{W_4(0) W_1(0)}} \right\}^{b_2} \tag{81b}$$

The relationships (75)–(81 a, b) show that the widths and the maximum positions of the spatial solitons (75) and (76) do not depend on their intensities, and they are determined by the pumping wave $\vec{E}_4$ intensity. They are strongly dependent on the correlation lengths corresponding to the interaction with the pumping and signal wave, respectively. The form and the position of the spatial solitons $W_{2,3}$ may be changed by the detuning of the coupled waves frequencies and by changing their propagation direction as well as by changing the pumping wave intensity. The validity of the approximations (66) and (67) requires

$$W_{1,4}(0) >> W_{2,3max}$$

According to the relationship (43) all coupling constants are of approximately the same order of magnitude, and consequently it is possible that

$$|a_{1,2}| << |b_{1,2}| \sim 1$$

The input pumping-signal ratio might not be too great, since for

$$W_4(0) >> W_1(0)$$

the constant pumping intensity approximation[1] is suitable. Numerical estimations show that in such a situation the condition (66) is satisfied with

$$W_{2,3}(0) \sim 10^{-2} W_4(0)$$

Combining the results (60)–(62), (75), (76) and taking into account the conservation law (73), we obtain two pairs of solutions for W_{11} and W_{41}:

$$(W_{11})_I = J_2 - W_2 - W_3 - (W_{41})_I \tag{82a}$$

$$(W_{41})_I = -\{\operatorname{sech}(\eta - \eta_1)\}^2 \int_0^{\eta} d\eta' \{1 + \exp[-2(\eta' - \eta_1)]\} \times \times \left\{ J_2 + W_2 \left(\frac{\beta_{42}}{\beta_{41}} - 1 \right) + W_3 \left(\frac{\beta_{43}}{\beta_{41}} - 1 \right) \right\} \tag{82b}$$

$$(W_{11})_{II} = \frac{1}{2} \{\operatorname{sech}(\eta - \eta_1)\}^2 \int_0^{\eta} d\eta' \{1 + \exp[2(\eta' - \eta_1)]\} \times \times \left\{ J_2 + W_2 \left(\frac{\beta_{21}}{\beta_{41}} - 1 \right) + W_3 \left(\frac{\beta_{31}}{\beta_{41}} - 1 \right) \right\} \tag{83a}$$

$$(W_{41})_{II} = J_2 - W_2 - W_3 - (W_{11})_{II} \tag{83b}$$

The existence of the solutions (82) and (83) means that the two levels of the intensity of the fundamental waves $E_{1,4}$ are possible:

$$W_1 = W_{10} + (W_{11})_{I,II}, \quad W_4 = W_{40} + (W_{41})_{I,II}$$

i.e. a specific kind of an optical dispersive bistability[36] occurs. The behaviour of the bistability in question may be evaluated qualitatively using the relationships (73)–(83a, b). Consider the solution (82a, b). Taking into account (75), (76) and (81a, b) we immediately obtain that

$$\eta \to \infty, \quad (W_{41})_I \to 0, \quad (W_{11})_I \to J_2 \tag{84}$$

To evaluate the second solution (83a, b) we divide the integration interval into two parts: $(0, \eta_0)$ and (η_0, η), where

$$\eta_0 >> \eta_{02,03}$$

is a sufficiently large constant number. The integrand in (83a) is finite for any finite η and an integral over the interval $(0, \eta_0)$ is a finite number, too. It does not exceed a value determined by the expressions (81a, b). As a result, the contribution to $(W_{11})_{II}$ due to this integral vanishes for $\eta \to \infty$. On the second part of the interval for sufficiently large η the contribution of $W_{2,3}$ to the integrand may be neglected according to the condition (78), and we obtain:

$$\lim_{\eta\to\infty}(W_{11})_{II}=\lim_{\eta\to\infty}\left\{\frac{1}{4}\left[\operatorname{sech}(\eta-\eta_1)\right]^2 J_2\exp\left[2(\eta-\eta_1)\right]\right\}=J_2,$$
$$\lim_{\eta\to\infty}(W_{41})_{II}=0 \tag{85}$$

It is seen from (84) and (85) that the initial states of each bistable kink at $z=0$ coincide as well as their behaviour at infinity. Usually such kind of bistability is caused by a deviation of the dependence of a refractive index on an intensity from Kerr type.[37, 38]

In our case the bistability is due to the combination of the specific kind of Kerr nonlinearity and of the essentially nondegenerate character of FWM when the matrix of different coupling constants emerges instead of one coupling constant. Indeed, if all β_{mn} are equal, the conservation law (73) is satisfied with the solutions (75), (76), (82b) and (83a), the solutions (82a, b) and (83a, b) coincide and the bistability vanishes.

It is seen from (84) and (85), that for large η the bistability vanishes. For small $\eta << \eta_1$ the bistability is determined mainly by the magnitude $[W_4(0)/W_1(0)]$ and by the anisotropy of the coupling constants β_{mn}. The dimensionless variable η is proportional to both the thickness of SmA and the pumping intensity. Keeping constant the sum input intensity J_1 we obtain that in SmA sample two points exist: $z=z_b$ where the bistability emerges, and $z=z_f>z_b$ where it vanishes. If, on the contrary, the thickness of SmA sample is fixed, then the levels of pumping corresponding to the threshold and to the completion of the bistability may in principle be determined equating for example the expressions (82b) and (83b) for some $z=d_b=\text{const}$.

Calculating the phases γ_m according to (42) we keep only $W_{10,40}$, neglecting small spatially localized quantities $W_{2,3}$ and corrections $W_{11,41}$. Substituting (60) into (42) we find:

$$\gamma_1=-\frac{1}{2}\frac{\delta_{14}}{\beta_{41}}\ln\left[\frac{\exp(\eta)\cosh(\eta_1)}{\cosh(\eta-\eta_1)}\right] \tag{86}$$

$$\gamma_2=-\frac{1}{2}\ln\left\{\exp\left[\frac{\delta_{21}+\delta_{24}}{\beta_{41}}\eta\right]\left[\frac{\cosh(\eta-\eta_1)}{\cosh(\eta_1)}\right]^{\mu_1}\right\} \tag{87}$$

$$\gamma_3 = -\frac{1}{2}\ln\left\{\exp\left[\frac{\delta_{31}+\delta_{34}}{\beta_{41}}\eta\right]\left[\frac{\cosh(\eta-\eta_1)}{\cosh(\eta_1)}\right]^{\mu_2}\right\} \tag{88}$$

$$\gamma_4 = -\frac{1}{2}\frac{\delta_{14}}{\beta_{41}}\ln\left[\frac{\exp(\eta)\cosh(\eta-\eta_1)}{\cosh(\eta_1)}\right] \tag{89}$$

where

$$\mu_1 = \frac{\delta_{21}-\delta_{24}}{\beta_{41}}, \quad \mu_2 = \frac{\delta_{31}-\delta_{34}}{\beta_{41}}$$

It is seen from (86)–(89) that the phase of the amplified wave $\vec{E}_1$ tends to the constant value, while the depletion of the waves $\vec{E}_4$ is accompanied by the almost periodical phase cross-modulation:

$$\eta \to \infty \qquad \gamma_1 \to -\frac{\delta_{14}}{2\beta_{41}}\ln\left[1+\frac{W_4(0)}{W_1(0)}\right], \qquad |\gamma_4| \to \infty$$

3.4. The Analog of BEFWM and the Phase Conjugation.

Consider the situation when the wave $\vec{E}_1$ is phase-conjugate of the wave $\vec{E}_4$, while the waves $\vec{E}_{2,3}$ are forward-going and backward-going pumping waves, respectively.[2] The phase-conjugate wave has the time-reversed phase factor with respect to the incident wave.[2] As a result, we obtain from the equation (15):

$$\vec{E}_1 = \vec{e}_1\left\{A_1 \exp i\left(\vec{k}_4\vec{r}+\omega_1 t\right) + c.c.\right\} \tag{90}$$

$$\vec{E}_2 = \vec{e}_2\left\{A_2 \exp i\left(\vec{k}_2\vec{r}-\omega_2 t\right) + c.c.\right\} \tag{91}$$

$$\vec{E}_3 = \vec{e}_3\left\{A_3 \exp i\left(\vec{k}_2\vec{r}+\omega_3 t + \Delta\vec{k}r\right) + c.c.\right\} \tag{92}$$

$$\vec{E}_4 = \vec{e}_4\left\{A_4 \exp i\left(\vec{k}_4\vec{r}-\omega_4 t\right) + c.c.\right\} \tag{93}$$

where $\Delta\vec{k}$ is the wave vector-mismatch of FWM process:[2]

$$\Delta\vec{k} = \Delta\vec{k}_{32} = \frac{\Delta\omega_{32}}{c}\vec{n}_3, \quad \vec{k}_3 = \frac{\omega_3}{c}\vec{n}_3 \tag{94}$$

$\vec{n}_3$ may be easily defined from the dispersion relations (18) or (19) for each kind of polarization. Comparing the relationships (2), (3), (20), (21) and (90)–(93) we see that for the counterpropagating waves $E_{1,4}$ and $E_{2,3}$ the products $E_4E_1^*$, $E_2E_1^*$,

$E_4E_3^*$ and $E_3E_2^*$ in (20) must be replaced by the products E_1E_4, E_1E_2, E_3E_4 and E_2E_3. Then the harmonics of the dynamic grating (20) take the form:

$$\begin{aligned} &U_{41} \sim A_1A_4 \exp i\left(2\vec{k}_4\vec{r} - \Delta\omega_{41}t\right), \quad U_{21} \sim A_1A_2 \exp i\left(\vec{k}^+\vec{r} - \Delta\omega_{21}t\right), \\ &U_{43} \sim A_4A_3 \exp i\left(\vec{k}^+\vec{r} - \Delta\omega_{43}t\right), \quad U_{32} \sim A_3A_2 \exp i\left(2\vec{k}_2\vec{r} + \Delta\omega_{32}t\right), \\ &U_{31} \sim A_1A_3^* \exp i\left(\vec{k}^-\vec{r} - \Delta\omega_{31}t\right), \quad U_{42} \sim A_2^*A_4 \exp i\left(\vec{k}^-\vec{r} - \Delta\omega_{42}t\right) \\ &\vec{k}^\pm = \vec{k}_4 \pm \vec{k}_2 \end{aligned} \tag{95}$$

In the case of the phase conjugation by stimulated scattering the condition of the frequency balance between the harmonics with the same wave vectors is necessary.[2] Choosing the frequency differencies

$$\Delta\omega_{21} = \Delta\omega_{43} = \Delta\omega_1 \tag{96}$$

and taking into account the conditions (2), (17) and (22)–(25) we obtain:

$$\begin{aligned} &\Delta\omega_{31} = \Delta\omega_{42} = \Delta\omega_2 > \Delta\omega_1 \\ &G_{21}\left(\Delta\omega_1, \quad \vec{k}^+\right) = G_{43}\left(\Delta\omega_1, \quad \vec{k}^+\right) = G^+ \\ &G_{31}\left(\Delta\omega_2, \quad \vec{k}^-\right) = G_{42}\left(\Delta\omega_2, \quad \vec{k}^-\right) = G^- \\ &h_{21} = h_{43} = h^+, \quad h_{31} = h_{42} = h^- \end{aligned} \tag{97}$$

The strongest coupling between EMW occurs in the resonant case when the condition (31) is met for one of the frequency differencies (96) and (97):

$$\Delta\omega_1 = \Omega\left(\vec{k}^+\right) = \Omega^+ \tag{98a}$$

$$\text{or} \quad \Delta\omega_2 = \Omega\left(\vec{k}^-\right) = \Omega^- \tag{98b}$$

Comparison of the relationships (31), (97) and (98a, b) shows that each of the resonances is possible only when the angle between $\vec{k}_2$ and $\vec{k}_4$ $\Theta > \pi/2$ and consequently $k^- > k^+$.

The contribution of the non-resonant harmonics may be neglected. Choose, for example, the case (98b). Then, assuming that the amplitudes of the forward-going and backward-going pumping waves $E_{2,3}$ are great in comparison with the probe and conjugated waves $E_{4,1}$ and they are kept constant

$$|A_{2,3}| >> |A_{1,4}|, \quad A_{2,3} = \text{const}$$

and combining the relationships (12), (20)-(25), (34), (35) and (90)–(98a,b) we obtain from the wave equation (33) the reduced equations for the amplitudes of the probe wave E and the conjugated wave E:

$$2l\frac{\partial A_1}{\partial r} = -\left(\frac{\omega_1}{c}\right)^2 \frac{1}{4\pi B}\left(\frac{h^-}{\Delta k_z^-}\right)^2 \frac{\Omega^-}{\Gamma^-}\times \times\left\{A_1|A_3|^2 + A_2^* A_3 A_4 \exp i\Delta\vec{k}\vec{r}\right\} \tag{99a}$$

$$2l\frac{\partial A_4}{\partial r} = -\left(\frac{\omega_4}{c}\right)^2 \frac{1}{4\pi B}\left(\frac{h^-}{\Delta k_z^-}\right)^2 \frac{\Omega^-}{\Gamma^-}\times \times\left\{A_4|A_2|^2 + A_1 A_2 A_3^* \exp\left(-i\Delta\vec{k}\vec{r}\right)\right\} \tag{99b}$$

where

$$l = k_4\left\{1 - \left(\vec{k}_4\vec{e}_1\right)^2 / k_4^2\right\}$$

The equations (99a, b) describe the enhanced FWM process with the simultaneous phase conjugation and the amplification of the conjugated wave E_1.[2,39] The equations (99a, b) are identical with the equations of BEFWM,[2,39] including the phase-matched terms responsible for the energy exchange and the phase-mismatched terms responsible for the phase conjugation. In the constant pumping approximation[1] the solutions of the system (99a, b) have the form

$$A_{1,4} = a_{1,4}\exp\left\{pr \pm i\Delta\vec{k}\vec{r}/2\right\} \tag{100}$$

Substituting (100) into (99a, b) we find the increment:

$$p_{1,2} = -\frac{1}{4l}\left(\frac{h^-}{\Delta k_z^-}\right)^2 \frac{\Omega^-}{\Gamma^-}\frac{\left[(\omega_4/c)|A_2|^2 + (\omega_1/c)^2|A_3|^2\right]}{4\pi B}\times \times\left\{1 \pm 1 \pm 2il\Delta k\left[(\omega_1/c)^2|A_3|^2 - (\omega_4/c)^2|A_2|^2\right]\times \times 4\pi B\frac{\Gamma^-}{\Omega^-}\left(\Delta k_z^-/h^-\right)^2\left[(\omega_1/c)^2|A_3|^2 + (\omega_4/c)^2|A_2|^2\right]^{-2}\right\} \tag{101}$$

$(Re\, p_1) < 0$, which corresponds to the amplification of the conjugated wave E_1 propagating in the negative direction. The increment $Re\, p_1$ coincides in general with the increment for the stimulated light scattering on SS.[21] Comparing $Re\, p_1$ with the coupling constant β_{mn} (43) we see that

$$|Re\, p_1| = \beta_{42}/2$$

if we take into account the conditions (95)–(98) and neglect the small intensities $|A_{1,4}|$. Therefore, the enhanced FWM with the phase conjugation process is a particular case of the more general model of the nearly degenerate parametric FWM on the cubic nonlinearity caused by smectic layer deformations.

4. THE GENERATION OF ADDITIONAL COMPONENTS AND SCATTERED HARMONICS.

The phase-matched components of the nonlinear polarization which are normal to the electric field of the fundamental EMW generate the additional field components.[1] If the fundamental EMW (15) are polarized in the layer plane and normal to the propagation direction, the only component of the nonlinear polarization which is normal to the field $\vec{E}_m$ is D^N_{mz} since SmA is a uniaxial crystal.[10] Combining the relationships (12), (18), (20), (21), (26) and (33)–(36), the condition[1,24]

$$\operatorname{div}\vec{D}_m = 0 \tag{102}$$

and projecting the corresponding part of the wave equation (33) on the direction $\vec{k}_m$, we obtain the equations for the additional components $\vec{E}'_m$:

$$-k_{mz}\left(\vec{k}_m\vec{E}'_m\right) + k^2_m E'_{mz} = \left(\frac{\omega_m}{c}\right)^2 D^N_{mz} \tag{103}$$

$$-\varepsilon_{\parallel}k_{mz}E'_{mz} - \varepsilon_{\perp}k_{m\perp}E'_{m\perp} = k_{mz}D^N_{mz} \tag{104}$$

where

$$D^N_{mz} = -\varepsilon_a A_m \exp i\left(\vec{k}_m\vec{r} - \omega_m t\right)\sum_n \frac{a_\perp}{4\pi B}\left(\vec{e}_m\vec{e}_n\right)\times \times\frac{|A_n|^2\Omega^2_{mn}\left(\Delta\vec{k}_{mn\perp}\vec{e}_{n\perp}\right)}{G_{mn}\Delta k_{mnz}} + c.c. \tag{105}$$

The solution of the system (103)–(104) yields

$$E'_{mz} = D^N_{mz}\frac{k^2_{m\perp}}{\varepsilon_\perp k^2_{m\perp} + \varepsilon_\parallel k^2_{mz}} \tag{106}$$

$$E'_{m\perp} = -D^N_{mz}\left(\frac{k_{mz}}{\varepsilon_\perp k_{m\perp}}\right)\frac{\varepsilon_\parallel k^2_m + \varepsilon_\perp k^2_{m\perp}}{\varepsilon_\perp k^2_{m\perp} + \varepsilon_\parallel k^2_{mz}} \tag{107}$$

If the fundamental EM waves (15) are polarized in the main cross-section, they propagate as the extraordinary ones with the dispersion relations (19).[24] Due to the anisotropy of SmA and the nonlinearity the transverse components of these EM waves emerge, which are polarized along the unit vectors

$$\vec{e}'_{m\perp} = [\vec{q}_m \times \vec{e}_m] / q_m \tag{108}$$

where $\vec{q}_m$ is a beam vector of the EMW $\vec{E}_m$, $\vec{q}_{m\perp}$ $\vec{e}_m$.[24] Projecting the corresponding part of the wave equation (33) on the direction $\vec{e}'_{m\perp}$ and using (19) we obtain

$$E'_{m\perp} = \frac{\omega_m^2}{q_m^2 c^2 k_m^2} \left(\vec{D}_m^N \cdot [\vec{q}_m \times \vec{e}_m] \right) \tag{109}$$

where $\vec{D}_m^N$ in this case is determined by the expressions (12), (19), (20)–(22) and (34). Comparing the relationships (105)–(107), (109) and (40) one may see that according to the conditions (51) and (52) all additional components E'_m are finite and spatially localized:

$$z \to \infty, \qquad E'_m \to 0 \tag{110}$$

The components of the nonlinear polarization (36) which are not phase-matched to the fundamental waves give rise to the number of the Brillouin-like scattered harmonics

$$\vec{f}_\ell^s = \vec{F}_\ell^s \exp i\psi_\ell \tag{111}$$

which evolve according to the corresponding wave equations:

$$\text{rot rot} \vec{f}_\ell^s + \frac{1}{c^2} \frac{\partial^2}{\partial t^2} \left(\varepsilon_\perp \vec{f}_{\ell\perp}^s + \varepsilon_\parallel f_{\ell z}^s \vec{z} \right) = -\frac{1}{c^2} \frac{\partial^2}{\partial t^2} \left(\vec{D}_\ell^N \exp i\psi_\ell \right) \tag{112}$$

Here ψ_ℓ are the phases of Stokes and anti-Stokes components[1] with the combination frequencies ω_ℓ and wave vectors $\vec{k}_\ell$ which are different from the fundamental ones. The combination frequencies and wave vectors do not satisfy the dispersion relations (18) or (19). Therefore the homogeneous solutions of (112) do not exist, and $\vec{f}_\ell^s$ are not the propagating modes.[19] They are driven by the nonlinear polarization in the right-hand side of (112). The amplitudes F_ℓ^s have the order of magnitude

$$F_\ell^s \sim \frac{\varepsilon_a^2 |A_p A_m A_n|}{4\pi B} \frac{\Omega_{mn}^2}{|G_{mn}|} \tag{113}$$

where $A_{p,mn}$ are the amplitudes of the fundamental waves (15). Comparing the expressions (40), (51), (52) and (113) it is seen that all harmonics f_ℓ^s have the finite and spatially localized amplitudes:

$$z \to \infty, \qquad |F_\ell^s| \to 0 \tag{114}$$

The total number of the scattered harmonics with essentially different frequencies and wave vectors is equal to 24. Indeed, the multiplication of 6 harmonics of the dynamic grating (20) and of the four fundamental EMW (15) yields 48 terms including 12 terms which are phase-matched to the fundamental waves (15). The remaining 36 terms include 12 terms of the type

$$A_m A_p A_n^* \exp i \left[\left(\vec{k}_m + \vec{k}_p - \vec{k}_n \right) \vec{r} - \left(\omega_m + \omega_p - \omega_n \right) t \right]$$

which are doubly degenerate, and 12 terms of the type

$$A_m^2 A_n^* \exp i \left[2 \left(\vec{k}_m \vec{r} - \omega_m t \right) - \left(\vec{k}_n \vec{r} - \omega_n t \right) \right]$$

5. THE HYDRODYNAMIC FLOW EXCITED BY THE STRONG OPTICAL FIELD.

The flexibility and sensitivity of liquid crystals with respect to the external fields are well known.[10–13] Hence it is important to investigate the influence of the strong optical field (15) on the hydrodynamic behaviour of SmA. In NLC the orientational motion of molecules gives rise to the so-called twist waves, or orientation waves without the hydrodynamic flow of the liquid as a whole.[26,27] In contrast, in SmA any disturbance in the layer displacement inevitably results in the hydrodynamic flow according to the equations (5) and (7). Substituting (20) and (21) into the equation (7) and using the incompressibility condition (5) we obtain

$$\begin{aligned} v_z &= \sum_{m\,n,\, m \neq n} V_{mn} \exp i \left(\Delta \vec{k}_{mn} \vec{r} - \Delta \omega_{mn} t \right) \\ v_x &= - \sum_{m,\, n,\, m \neq n} \left[V_{mn} \exp i \left(\Delta \vec{k}_{mn} \vec{r} - \Delta \omega_{mn} t \right) \right] \frac{\Delta k_{mnz}}{\Delta k_{mnx}} \\ V_{mn} &= A_m A_n^* \frac{\Delta \omega_{mn} h_{mn} \Omega_{mn}^2}{4\pi B G_{mn} (\Delta k_{mnz})^2} \end{aligned} \tag{115}$$

The hydrodynamic flow (115) is a complicated spatio-temporal pattern[28] which represents a superposition of 6 harmonics with different spatial scales $\sim (\Delta k_{mn})^{-1}$ and temporal periods $\sim (\Delta\omega_{mn})^{-1}$. According to the relationships (3), (4), (18) and (19)

$$k_m \sim k_n$$

For the small angles between $\vec{k}_m$ and $\vec{k}_n$

$$\Delta k_{mn} << k_m$$

and $\Delta\vec{k}_{mn}$ is approximately normal to the propagation directions of the coupled EMW (15). Consequently, the direction of the hydrodynamic velocity $\vec{v}$ would approximately coincide with the EMW propagation direction. If additionally the angle between $\vec{k}_{m,n}$ and the Z axis is also small, then

$$|v_z| >> |v_x|$$

and SmA would mainly flow in the direction normal to the layer. In the opposite case, when EM waves propagate under a small angle to a layer plane they give rise to the flow which is almost parallel to the layer plane. Each harmonic may be characterized by two spatial scales: the short scale is determined by the inverse wave vector $(\Delta k_{mn})^{-1}$, while the large scale is due to the spatial inhomogeneity of the amplitudes A_m and it is determined by the correlation lengths $(\beta_{mn})^{-1}$. Substituting the relationships (23), (40) and (43) into (115) we obtain:

$$|V_{mn}|^2 = M_{mn}\beta_{mn}\frac{I_0}{4\pi B}\frac{\Omega_{mn}^2\Delta\omega_{mn}}{(\Delta k_{mnz})^2\,\Gamma_{mn}} \tag{116}$$

where

$$M_{mn} = W_m W_n = W_m(0)W_n(0)\exp\left\{-\int_0^z\left(\sum_j \beta_{mj}W_j + \sum_i \beta_{ni}W_i\right)dz'\right\} \tag{117}$$

The factor M_{mn} in the right-hand side of (116) determines the large-scale profile of the hydrodynamic velocity, while the combination of the energetic, temporal and spatial parameters yields its magnitude. Comparing the expressions

(117) and (50)–(52) we see that all amplitudes V_{mn} are finite and spatially localized:

$$z \to \infty, \qquad |V_{mn}| \to 0 \tag{118}$$

Therefore all hydrodynamic excitations (115) are convective.[29] $|V_{mn}|$ may have a maximum determined by the condition

$$\sum_j \beta_{mj} W_j(z_0) + \sum_i \beta_{ni} W_i(z_0) = 0$$

It is clear that all points of the maxima $z_{0mn} > 0$ exist, if there exist the points z_{02}, $z_{03} > 0$ determined by the conditions (47), (48) and the crossing-point $z_1 > 0$ where

$$\int_0^{z_1} \left\{ \sum_j \beta_{j1} W_j + \sum_i \beta_{4i} W_i \right\} dz' = \ln \left[\frac{W_4(0)}{W_1(0)} \right]$$

Consequently, the hydrodynamic velocity harmonics have the envelopes in the form of spatial solitons,[25] which are oblique to the propagation direction. In the particular case, when $W_{1,4} >> W_{2,3}$ using the results (60), (75)–(77) and (79a, b) we find:

$$\begin{aligned}
M_{14} &= \frac{1}{4} J_1^2 \left[\operatorname{sech}(\eta - \eta_1)\right]^2 >> M_{mn} \\
M_{12,42} &= \frac{1}{2} J_1 W_2(0) \exp(a_1 \eta) \left[\frac{\cosh(\eta_1)}{\cosh(\eta - \eta_1)} \right]^{b_1} \times \left[1 \pm \tanh(\eta - \eta_1)\right] \\
M_{13,43} &= \frac{1}{2} J_1 W_3(0) \exp(a_2 \eta) \left[\frac{\cosh(\eta_1)}{\cosh(\eta - \eta_1)} \right]^{b_2} \left[1 \pm \tanh(\eta - \eta_1)\right] \\
M_{23} &= W_2(0) W_3(0) \exp\left\{(a_1 + a_2)\eta\right\} \left[\frac{\cosh(\eta_1)}{\cosh(\eta - \eta_1)} \right]^{b_1 + b_2}
\end{aligned} \tag{119}$$

The analysis of the expressions (119) shows that they have the form of a spatial soliton,[25] with the following points of a maximum: M_{14} has the maximum at the crossing-point $\eta = \eta_1$. The solitons $M_{12,42}$ and $M_{13,43}$ have their maxima at the points

$$\begin{aligned}
\eta_{012} &= \eta_1 + \frac{1}{2} \ln \left(\frac{\beta_{42} + \beta_{41}}{\beta_{21}} \right), \\
\eta_{042} &= \eta_1 - \frac{1}{2} \ln \left(\frac{\beta_{41} + \beta_{21}}{\beta_{42}} \right), \\
\eta_{013} &= \eta_1 + \frac{1}{2} \ln \left(\frac{\beta_{43} + \beta_{41}}{\beta_{31}} \right), \\
\eta_{043} &= \eta_1 - \frac{1}{2} \ln \left(\frac{\beta_{41} + \beta_{31}}{\beta_{43}} \right)
\end{aligned} \tag{120}$$

The smallest soliton M_{23} has its maximum at the point

$$\eta_{023} = \eta_1 + \frac{1}{2}\ln\left(\frac{\beta_{42}+\beta_{43}}{\beta_{21}+\beta_{31}}\right) \tag{121}$$

It is seen from the expressions (119)–(121) that the hydrodynamic flow is divided into the large-scale strata with the different temporal and short-scale spatial periodicity. If all β_{mn} are essentially different, the points η_{0mn} would be well resolved one from another and the different strata (119) would be distributed approximately symmetrically in respect to the maximum of the largest component V_{14}. In the opposite case when all β_{mn} are approximately equal the small components V_{mn} with the rapidly oscillating different phases may be neglected in comparison with V_{14}, and the hydrodynamic flow would have the soliton profile M_{14}. Numerical estimations show that all $|V_{mn}|$ vanish for $\eta \sim (4-5)$. Each amplitude $|V_{mn}|$ reaches its maximal value in the resonant case when the condition (31) is met. Taking into account the expressions (1), (2), (18) or (19), (22)–(24), (40) and (53) we obtain:

$$|V_{mn}^{res}| \sim (M_{mn})^{\frac{1}{2}}\, s|\beta_{mn}^{res}|(\omega/c)^{-1}\,\frac{\sqrt{\varepsilon_\perp\varepsilon_\|}}{|\varepsilon_a|} \tag{122}$$

Using the results of section 3.1 we find that the hydrodynamic velocity may reach a maximal value of about 10 cm sec^{-1}. The minimal sample thickness d_s sufficient for the excitation of the hydrodynamic spatial soliton (119) in the strong optical field must be of the order of magnitude of the excitation (correlation) length $L_E \sim 0.02$ cm. The SmA samples of a thickness $\sim (200-500)\,\mu$m were used to observe the stimulated light scattering and the SS excitation in SmA.[33,40,41]

The results obtained are valid for both homeotropically and planary oriented[10] SmA. The only necessary condition is that EMW would propagate obliquely to the layers, or in other words, to the optical axis of SmA.

6. THE LIGHT-INDUCED LONGITUDINAL WAVES OF THE HIGH-FREQUENCY ELECTRIC FIELD.

It is known that in SmA the layer deformations give rise to the so-called flexoelectric polarization $\vec{P}_f$,[15,31] which has the form:[15]

$$P_{fx} = -e_3^f \frac{\partial^2 u}{\partial z \partial x},$$
$$P_{fy} = -e_3^f \frac{\partial^2 u}{\partial z \partial y} \tag{123}$$
$$P_{fz} = -e_1^f \left(\frac{\partial^2 u}{\partial x^2} + \frac{\partial^2 u}{\partial y^2} \right) - e_2^f \frac{\partial^2 u}{\partial z^2}$$

where $e^f_{1,2,3}$ are the flexoelectric coupling constants. The polarization (123), in turn, causes the electric field $\vec{E}_f$ according to the condition:[24]

$$\operatorname{div}\left(\varepsilon_\perp \vec{E}_{f\perp} + \varepsilon_\parallel E_{fz}\vec{z} + 4\pi \vec{P}_f\right) = 0 \tag{124}$$

The magnetic field $\vec{H}_f$ associated with the flexoelectric polarization $\vec{P}_f$ caused by the dynamic grating (20) is small and may be neglected:

$$H_f \sim \frac{1}{c}\frac{\Delta\omega}{\Delta k} P_f \sim \frac{s}{c}\frac{k_m}{\Delta k_{mn}} P_f << P_f$$

Therefore the electric field $\vec{E}_f$ generated by the dynamic grating due to the flexoelectric effect[10,15,31] is longitudinal:[30]

$$\operatorname{rot}\vec{E}_f = 0 \tag{125}$$

Combining the equations (20), (21) and (123)–(125) we obtain:

$$\begin{aligned} \vec{E}_f = -\frac{i}{B} \sum_{m,n,m\neq n} & \frac{h_{mn}\Delta\vec{k}_{mn}\Omega^2_{mn}}{\Delta k_{mn} G_{mn}} A_m A_n^* \times \\ & \times \left\{ \left(e_1^f + e_3^f\right) \frac{(\Delta k_{mn\perp})^2}{\Delta k_{mn}\Delta k_{mnz}} + e_2^f \Delta k_{mnz}/\Delta k_{mn} \right\} \times \\ & \times \exp i\left(\Delta\vec{k}_{mn} r - \Delta\omega_{mn} t\right) \end{aligned} \tag{126}$$

The longitudinal electric field $\vec{E}_f$ is spatially localized. Comparing the expressions (40), (51) (52) and (126) it is seen that E_f vanishes at sufficiently large distances:

$$z \to \infty, \qquad |E_f| \to 0 \tag{127}$$

Each harmonic in the sum (126) differs from the corresponding harmonic of the dynamic grating (20) by a factor and has the same resonant form. At the interface $z = 0$ the terms E_{fmn} behave as high-frequency spatially periodic surface waves, since they cannot penetrate into the linear medium $z < 0$. Actually, according to the boundary conditions[24] the tangential component of the wave vector of each harmonic (126) is continuous at $z = 0$:

$$k^L_{mn\perp} = \Delta k_{mn\perp}$$

The normal component k^L_{mnz} is purely imaginary, since

$$\left(\omega_{mn}/c\right)^2 \sim (s/c)^2 k_m^2 << (\Delta k_{mn\perp})^2 \sim k_m^2 \sin^2(\theta/2)$$

and therefore

$$\left(k^L_{mnz}\right)^2 = \left(\Delta\omega_{mn}/c\right)^2 - \left(\Delta k_{mn\perp}\right)^2 < 0$$

The high-frequency electric field with artificially created periodicity at the interface $z = 0$ excites SS when being applied to SmA sample.[40,41] The equation (126) shows that the inverse effect is possible when the light-induced dynamic grating of smectic layer displacement excites a wave packet of spatially periodic high-frequency longitudinal electric field.

7. CONCLUSIONS.

The nondegenerate FWM in SmA results in an excitation of the dynamic grating of a layer displacement and in an energy exchange among the coupled EM waves due to a new type of Kerr nonlinearity caused by the layer deformations. The necessary conditions for a strong coupling are as follows:

1. the difference between the EM wave frequencies is of the same order of magnitude as SS frequency;
2. the EM waves propagate obliquely to a layer.

The cubic susceptibility determined by the layer deformations represent the fourth rank tensor with essentially complex components exhibiting a spatial dispersion on the dynamic grating wave vectors. The explicit expression of the cubic susceptibility is presented in Appendix A. The eigenmodes of SS are not excited, since the excitation length for the energy exchange among the coupled waves is much greater than SS dissipation length. As a result, SmA behaves like an elastic channel for energy transfer from the EMW with greater frequencies to the EMW with lower frequencies. The analysis carried on in SVA approximation shows that in general case a combination of the nonlinearity and spatial dispersion results in an excitation of the stable spatially localized structures. The EMW with the lowest frequency is amplified with a saturation at large distances. The EMW with the greatest frequency is depleted. The EMW with intermediate frequencies form the soliton-like structures. It is shown that the system of the coupled EMW and dynamic grating is stable with respect to the increase of a SmA sample thickness, as well as of a pumping intensity.

If the input pumping-signal intensity ratio is sufficiently large, only a limited interval exists where three waves with lower frequencies are amplified. The explicit expressions of the intensities and phases of the waves are obtained for some particular cases. The amplitudes have a form of kinks and spatial solitons. It is shown that in the special case of the geometry typical for a phase conjugation process an analog of BEFWM[2,7–9] occurs with the amplification of the conjugated wave. The nonlinearity and the existence of different excitation (correlation) lengths give rise to the specific kind of dispersive optical bistability, which usually occurs in media with deviations from Kerr nonlinearity.[38,38] The combination of nonlinearity and anisotropy results in the generation of additional components of the fundamental EMW. The scattering of the fundamental EMW on the dynamic grating generates the spectrum of Brillouin-like small harmonics with the combination frequencies and wave vectors.

Unlike NLC, in SmA a time-dependent orientational disturbance connected with a layer displacement ultimately results in the excitation of a hydrodynamic flow. This flow represents a complicated spatio-temporal pattern[28] with two different spatial scales. The short scale is determined by the wave vector of the dynamic gratind harmonics. The large scale is associated with the energy exchange between the EMW, and it is characterized by excitation (correlation) lengths. All components of the hydrodynamic velocity are spatially localized.

In liquid crystals the orientational disturbances generate an electric field due to the flexoelectric effect.[10,15,31] It is shown that the light-induced dynamic grating generates a longitudinal high-frequency electric field, which behaves as a surface wave at the boundary between SmA and a linear medium.

The numerical estimations for the typical values of material parameters and for the pumping intensity $\mathcal{P} \sim 100\,\mathrm{MW/cm^2}$ yield the gain coefficient $\beta \sim (15-50)$

cm^{-1}. This value corresponds to the excitation length of about (0.02 – 0.07) cm and agrees with the experimental data.[33] The hydrodynamic velocity may reach a value of 10 cm/sec .

APPENDIX A.

In general case the layer deformations break the symmetry of SmA.[7] Therefore, new components of the cubic susceptibility emerge in comparison with the intrinsic cubic susceptibility of the electron origin.[1] Comparing the relationships (21), (22) and (28) we find:

$$\left(\chi_{mn}^{(3)}\right)_{zzzz} = \chi_{mn\|}^{(3)} = -a_{\|}^{2} S_{mn} \left(\Delta k_{mnz}\right)^{2} \tag{A1}$$

$$\left(\chi_{mn}^{(3)}\right)_{xxxx} = \left(\chi_{mn}^{(3)}\right)_{yyyy} = \left(\chi_{mn}^{(3)}\right)_{\perp} = -a_{\perp}^{2} S_{mn} \left(\Delta k_{mnz}\right)^{2} \tag{A2}$$

$$\begin{aligned}\left(\chi_{mn}^{(3)}\right)_{zzzx} = \left(\chi_{mn}^{(3)}\right)_{zzxz} = \left(\chi_{mn}^{(3)}\right)_{xzzz} = \left(\chi_{mn}^{(3)}\right)_{zxzz} = \\ = \varepsilon_a a_{\|} S_{mn} \left(\Delta k_{mnz}\right)\left(\Delta k_{mnx}\right)\end{aligned} \tag{A3}$$

$$\begin{aligned}\left(\chi_{mn}^{(3)}\right)_{zzzy} = \left(\chi_{mn}^{(3)}\right)_{zzyz} = \left(\chi_{mn}^{(3)}\right)_{yzzz} = \left(\chi_{mn}^{(3)}\right)_{zyzz} = \\ = \varepsilon_a a_{\|} S_{mn} \left(\Delta k_{mnz}\right)\left(\Delta k_{mny}\right)\end{aligned} \tag{A4}$$

$$\left(\chi_{mn}^{(3)}\right)_{zzxx} = \left(\chi_{mn}^{(3)}\right)_{zzyy} = -a_{\|} a_{\perp} S_{mn} \left(\Delta k_{mnz}\right)^{2} \tag{A5}$$

$$\begin{aligned}\left(\chi_{mn}^{(3)}\right)_{xzxz} = \left(\chi_{mn}^{(3)}\right)_{zxxz} = \left(\chi_{mn}^{(3)}\right)_{xzzx} = \left(\chi_{mn}^{(3)}\right)_{zxzx} = \\ = -\varepsilon_a^{2} S_{mn} \left(\Delta k_{mnx}\right)^{2}\end{aligned} \tag{A6}$$

$$\begin{aligned}\left(\chi_{mn}^{(3)}\right)_{zyzy} = \left(\chi_{mn}^{(3)}\right)_{zyyz} = \left(\chi_{mn}^{(3)}\right)_{yzzy} = \left(\chi_{mn}^{(3)}\right)_{yzyz} = \\ = -\varepsilon_a^{2} S_{mn} \left(\Delta k_{mny}\right)^{2}\end{aligned} \tag{A7}$$

$$\begin{aligned}\left(\chi_{mn}^{(3)}\right)_{zxzy} = \left(\chi_{mn}^{(3)}\right)_{zyzx} = \left(\chi_{mn}^{(3)}\right)_{xzyz} = \left(\chi_{mn}^{(3)}\right)_{xzzy} = \\ = \left(\chi_{mn}^{(3)}\right)_{yzzx} = \left(\chi_{mn}^{(3)}\right)_{xyxz} = -\varepsilon_a^{2} S_{mn} \left(\Delta k_{mnx}\right)\left(\Delta k_{mny}\right)\end{aligned} \tag{A8}$$

$$\begin{aligned}\left(\chi_{mn}^{(3)}\right)_{xxxz} = \left(\chi_{mn}^{(3)}\right)_{xxzx} = \left(\chi_{mn}^{(3)}\right)_{xzxx} = \left(\chi_{mn}^{(3)}\right)_{zxxx} = \\ = \varepsilon_a a_{\perp} S_{mn} \left(\Delta k_{mnz}\right)\left(\Delta k_{mnx}\right)\end{aligned} \tag{A9}$$

$$\begin{aligned}\left(\chi_{mn}^{(3)}\right)_{yyyz} = \left(\chi_{mn}^{(3)}\right)_{yyzy} = \left(\chi_{mn}^{(3)}\right)_{yzyy} = \left(\chi_{mn}^{(3)}\right)_{zyyy} = \\ = \varepsilon_a a_{\perp} S_{mn} \left(\Delta k_{mnz}\right)\left(\Delta k_{mny}\right)\end{aligned} \tag{A10}$$

has its maximal value in the resonant case when the condition (31) is met. Using the relationships (1), (2), (23)–(25) and (30) we obtain:

$$\left|\chi^{(3)}_{mn}\right| \sim \frac{1}{4\pi B}\frac{\Omega}{\Gamma}\varepsilon_a^2 \tag{A11}$$

For the typical values of material parameters,[10,13,17,40,41] small angles θ between $\vec{k}_m$ and $\vec{k}_n$, and $k_m \sim 5 \cdot 10^4$ cm^{-1} we find that $\Delta k_{mn} \sim (10^3 - 5 \cdot 10^3)$ cm^{-1} and $|\chi^{(3)}_{mn}| \sim (10^{-9} - 10^{-8})$ cm^3/erg, which is comparable with the Brillouin nonlinearity in organic liquids.[1]

ACKNOWLEDGEMENTS.

One of the authors (B. Lembrikov) is very grateful to the "Bat Sheva de Rothschild Foundation for the Advancement of Science in Israel" for the financial support of this work.

REFERENCES.

1. Y.R. Shen, The principles of Nonlinear Optics (John Wiley and Sons, New York, 1984), pp. 242, 247-254, 42-44, 47-49, 303-304, 330.
2. Robert W. Boyd and Gilbert Grynberg, Contemporary Nonlinear Optics, edited by Govind P. Agrawal and Robert Boyd (Academic Press, New York, 1992), Chap. 3, pp. 86-106.
3. Y. Chen and Allan W. Snyder, Optics Letters, 14, 87 (1989).
4. Y. Chen, J. Opt. Soc. Am. B, 6, 1986 (1989).
5. B. Kryzhanovsky, A. Karapetyan and Boris Glushko, Phys. Rev. A, 44, 6036 (1991).
6. B. Kryzhanovsky and Boris Glushko, Phys. Rev. A, 45, 4979 (1992).
7. A.M. Scott and K.D. Ridley, IEEE J. Quantum Electron., 25, 438 (1989).
8. W.A. Schroeder, M.J. Damzen, and M.H.R. Hutchinson, IEEE J. Quantum Electron., 25, 460 (1989).
9. V.F. Efimkov, I.G. Zubarev, S.A. Pastukhov, and V.B. Sobolev, Sov. J. Quantum Electron., 22, 62 (1992).
10. P.G. De Gennes, The Physics of Liquid Crystals (Clarendon Press, Oxford, 1974), Chap. 1, pp. 13-14, Chap. 7, pp. 273, 284, 295, 301-307.
11. S.M. Arakelyan, G.A. Lyakhov, and Yu.S. Chilingaryan, Sov. Physics Uspechi, 23, 245 (1980).
12. B. Ya. Zel'dovich and N.V. Tabiryan, N.V., Sov. Phys. Uspechi, 28, 1059 (1985).
13. I.C. Khoo, in Progress in Optics, edited by Emil Wolf (North Holland, Amsterdam, 1988), vol. 26, pp. 108, 115, 127.
14. N.V. Tabiryan and B.Ya. Zel'dovich, Mol. Cryst. Liq. Cryst., 69, 31 (1981).

15. P.G. de Gennes, J. Phys. Paris, Colloque, 30, C4-65 (1969).
16. P.C. Martin, O. Parodi and P.S. Pershan, Phys. Rev. A, 6, 2401 (1972).
17. M.J. Stephen and J.P. Straley, Rev. Mod. Phys., 47, 617 (1974).
18. S. Chandrasekhar, Liquid Crystals (Cambridge University Press, Cambridge, 1977), Chap. 5, pp. 297-304.
19. L.D. Landau and E.M. Lifshitz, Theory of Elasticity, (Third Edition) (Pergamon Press, Oxford, 1987), Chap. 6, pp. 179-184, Chap. 3, p. 105.
20. B.I. Lembrikov, Sov. Physics Technical Physics, 25, 1145 (1980).
21. B.I. Lembrikov, Sov. Physics Solid State, 23, 715 (1981).
22. B.I. Lembrikov, Sov. Physics Technical Physics, 27, 923 (1982).
23. G.F. Kventsel and B.I. Lembrikov, Liquid Crystals, 16, 159 (1994).
24. L.D. Landau and E.M. Lifshitz, Electrodynamics of Continuous Media (Second edition) (Pergamon Press, Oxford, 1984), Chap. 12, p. 358, Chap. 2, pp. 35, 54-55, Chap. 11, pp. 333-340, Chap. 9, p. 257, Chap. 10, pp. 293-294.
25. R.K. Dodd, J.C. Eilbeck, J.D. Gibbon, and H.C. Morris, Solitons and Nonlinear Wave Equations (Academic Press, London, 1984), Chap. 1, pp. 31-33, Chap. 10, p. 587.
26. A. Saupe, Mol. Cryst. Liq. Cryst., 7, 59 (1969).
27. J.L. Ericksen, Mol. Cryst. Liq. Cryst., 7, 153 (1969).
28. M.C. Cross and P.C. Hohenberg, Rev. Mod. Phys., 65, 851 (1993), Chap. 7, pp. 940-941.
29. E.M. Lifshitz and L.P. Pitaevskii, Physical Kinetics (Pergamon Press, Oxford, 1981), Chap. 6, pp. 268-276.
30. L.D. Landau and E.M. Lifshitz, The Classical Theory of Fields (fourth edition) (Pergamon Press, Oxford, 1989), Chap. 6, p. 125.
31. J. Prost and P.S. Pershan, J. Appl. Phys. (USA), 47, 2298 (1976).
32. I.C. Khoo and R. Normandin, J. Appl. Phys. (USA), 55, 1416 (1983).
33. I.C. Khoo, Robert R. Michael and P.Y. Yan, IEEE Journal of Quant. Electronics, QE-23, 1344 (1987).
34. I.C. Khoo, R.G. Lindquist, R.R. Michael, R.J. Mansfield, and P. LoPresti, J . Appl. Phys. (USA), 69, 3853 (1991).
35. G.A. Korn, T.M. Korn, Mathematical Handbook (McGraw-Hill, New York, 1968), Chap. 1, pp. 24-27, Chap. 9, p. 253.
36. Hyatt M. Gibbs, Optical Bistability: Controlling Light with Light (Academic Press, New York, 1985), Chap. 1.1.
37. F.G. Bass, V.V. Konotop and S.A. Puzenko, Phys. Rev. A, 46, 4185 (1992).
38. Wieslaw Krolikowski, Nail Akhmediev and Barry Luther-Davies, Phys. Rev. E, 48, 3980 (1993).
39. G. Rivoire, J.L. Ferrier, J. Gazengel, J.P. Lecoq, and N. Xuan, Optics Comm., 48, 143 (1983).
40. L. Ricard and J. Prost, J. Phys. Paris, Colloque, 40, C3-83 (1979).
41. L. Ricard and J. Prost, J. Phys. Paris, 42, 861 (1981).